

## CONFORMATIONAL ANALYSIS OF ANTITUMOR CYCLIC HEXAPEPTIDES, RA SERIES<sup>1)</sup>

Hiroshi Morita,<sup>a</sup> Kazuyuki Kondo,<sup>a</sup> Yukio Hitotsuyanagi,<sup>a</sup> Koichi Takeya,<sup>a</sup> Hideji Itokawa,<sup>\*a</sup>  
 Nobuo Tomioka,<sup>b</sup> Akiko Itai,<sup>b</sup> and Yoichi Iitaka<sup>c</sup>

Department of Pharmacognosy, Tokyo College of Pharmacy,<sup>a</sup> Horinouchi 1432-1, Hachioji, Tokyo 192-03,  
 Japan, Faculty of Pharmaceutical Sciences, University of Tokyo,<sup>b</sup> Hongo, Bunkyo-ku, Tokyo 113, Japan and  
 Faculty of Medicine, Teikyo University,<sup>c</sup> Ohtsuka 359, Hachioji, Tokyo 192-03, Japan

(Received in Japan 10 November 1990)

**Abstract :** Conformational analysis of an antitumor cyclic hexapeptide, RA and its analogues isolated from *Rubia akane* and *R. cordifolia* was conducted by the spectroscopic and computational chemical methods. A combination of different homo- and heteronuclear two-dimensional NMR techniques at 500MHz have enabled us to perform complete assignment of the <sup>1</sup>H and <sup>13</sup>C signals of the two conformers A and B of RA-VII in CDCl<sub>3</sub>. The structures of the three conformers (A, B and C) in DMSO-d<sub>6</sub> were also determined by 2D-NMR techniques, temperature effects on NH protons and NOE experiments. Distances deduced from the NMR measurements were used for the refinements by the restrained molecular dynamics calculations using AMBER program. These conformational analysis showed that these conformers were caused by geometrical isomerization and that the predominant conformer A exhibits a typical type II β-turn structure, which is similar to the crystal structure analyzed by the X-ray diffractions. The reduced biological activity of the N-methyl derivative of RA-VII in comparison to RA-VII may be responsible for the more weakly populated conformer A in solution. Further, the presence of a highly strained 14-membered ring was necessary to maintain the typical type II β-turn structure of conformer A, and the ring system and turn structure were considered to play an important role in its antitumor activity.

### Introduction

A series of bicyclic hexapeptides, named RAs are potent antitumor compounds isolated from Rubiac Radix (roots of *Rubia cordifolia* and *R. akane*).<sup>2)</sup> Their structures,<sup>3)</sup> physiological activities<sup>4)</sup> and also total synthesis of RA-VII<sup>5)</sup> have been reported. As shown in Figure 1, the bicyclic hexapeptides of RAs contain both 18 membered-ring and 14 membered-ring systems with unique isodityrosine structures and the main active principle, RA-VII, contains three N-methyl-O-

methyl-L-tyrosine, two L-alanine and a D-alanine. These compounds are noted as new type anticancer agents having not only the unique bicyclic structure but also the unique action primarily to inhibit the protein synthesis.<sup>6)</sup> Various studies of the structure-activity relationships<sup>7)</sup> showed that its biological activity is reduced when a large substituent is introduced to the α-site of Tyr-6-Cβ. Since Kriek et al.<sup>8)</sup> reported that

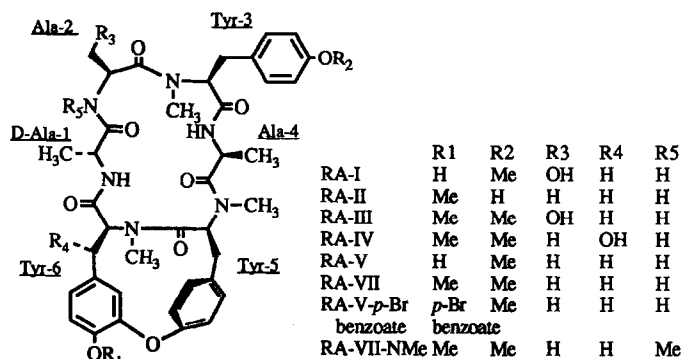


Figure 1  
 Structure of RAs; The amino-acid residues were abbreviated by their conventional three-letter notations, i.e. Ala=alanine, Tyr=N-methyl-O-methyl-tyrosine, D-Ala=D-alanine.

hexapeptides lacking a diphenyl ether bond were devoid of antitumor activity, the 14 membered ring containing an ether group seemed to be very important for the biological activity.

The  $^1\text{H-NMR}$  spectrum of RA-VII suggested the presence of two stable conformational states in  $\text{CDCl}_3$ , i.e. conformers A and B, and of three different conformers A, B and C in a polar solvent, for example, in  $\text{DMSO-d}_6$ , which could also result from isomerization about one or several of the amide bonds with isomerization rate slow enough to give separate signals in the NMR. The ratio of these conformers at equilibrium varies in different solutions (Table 1). Further, the N-mono methylated derivative of RA-VII (RA-VII-NMe) giving a conformer composition different from that of RA-VII showed a reduced effect against P-388 leukemia.

Table 1 Percent of the conformers of RA-VII and RA-VII-NMe in various solutions

Compound	solvent	conformer A (%)	B (%)	C (%)
RA-VII	$\text{CDCl}_3$	88.6	11.4	
	$\text{DMSO-d}_6$	63.7	31.8	4.5
	Dioxane-d <sub>8</sub>	79.2	20.8	
	30%DMSO-d <sub>6</sub> /D <sub>2</sub> O	76.0	24.0	
RA-VII-NMe	$\text{CDCl}_3$	77.3	21.2	1.6
	$\text{DMSO-d}_6$	57.1	25.3	17.6
	Dioxane-d <sub>8</sub>	47.1	44.4	8.5
	30%DMSO-d <sub>6</sub> /D <sub>2</sub> O	64.0	36.0	

Conformational analysis of flexible biomolecules<sup>9)</sup> is quite interesting because many cyclic and linear peptides are considered not to be rigid in solution. So, we studied the correlation between the conformations and pharmacological properties of such compounds by the analysis of each conformer A, B and C of RA-VII and RA-VII-NMe. The combination of 2D-NMR analysis with molecular dynamics and mechanics calculations led us to a complete assignment of each conformer and the conformations of complex molecules in solution. Here we report on the conformational analysis of RA series in solid and solution states by spectroscopic (NMR, CD and X-ray analysis) and computational chemical methods (molecular dynamics and molecular mechanics calculation).

### Crystalline structure of RA-V-*p*-bromobenzoate<sup>10)</sup>

Figure 2 shows the backbone of this cyclic peptide in a stereoscopic view. In Figure 3, the  $\phi$  and  $\psi$ -angles are summarized in the Ramachandran plot, which shows that all ( $\phi, \psi$ )-values lie in the  $\beta$ -region allowed for L-amino acids with the exception of the ( $\phi, \psi$ )-value for Tyr-3 which is in the left handed  $\alpha$ -helix region. D-Ala-1, however, is in the ( $\phi, \psi$ )-space accessible only by D-amino acids. As indicated in Figure 2, the cyclic peptide can be divided into two structurally distinct moieties: one, the more characteristic moiety is a highly strained 14 membered ring consisting of a diaryl ether, Tyr-5 and

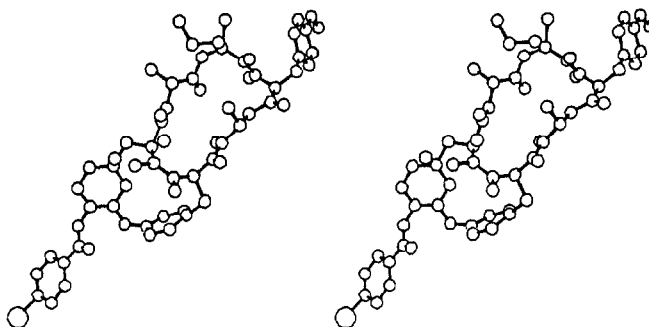


Figure 2 Stereoscopic view of RA-V-*p*-bromobenzoate  
 Crystal data:  $\text{C}_{47}\text{H}_{51}\text{N}_6\text{O}_{10}\text{BrC}_2\text{H}_5\text{OH}2\text{H}_2\text{O}$ , Monoclinic, space group  $\text{P2}_1$ ,  
 $z=2$ ,  $a=27.8741(15)$ ,  $b=9.653(6)$ ,  $c=9.758(6)\text{\AA}$ ,  $\beta=95.77(6)^\circ$ ,  $V=2612\text{\AA}^3$ ,  
 $R=0.096$ .

Tyr-6, and the other is 18 membered ring which forms an antiparallel  $\beta$ -pleated sheet with a type II  $\beta$ -turn at residues Ala-2 and Tyr-3. These

Table 2 Lengths ( $\text{\AA}$ ) of hydrogen bondings of calculated conformers A and B of RA-VII and RA-VII-NMe (See Molecular dynamics and energy minimization), and X-ray structure of RA-V-p-bromobenzoate

Hydrogen bridge Donor	Hydrogen bridge Acceptor	X-ray	Conformer A (RA-VII)	B	A (RA-VII-NMe)	B (RA-VII-NMe)
Ala-4-NH	D-Ala-1-O	2.954	2.285	1.984	2.459	2.132
D-Ala-1-NH	Ala-4-O	3.238	2.215	2.213	2.219	2.119

constituent residues are rarely found in classical type II  $\beta$ -turns because there is steric repulsion between the carbonyl moiety of  $i+1$  and side chain of  $i+2$ . In other words, each Ala-Tyr sequences may form type II  $\beta$ -turn if the Tyr residue is D-amino acid residue.<sup>11</sup> Moreover, two weak intramolecular H-bonds between Ala-4-NH and D-Ala-1-O ( $\text{NH4}\cdot\text{O1}$ ), and D-Ala-1-NH and Ala-4-O ( $\text{NH1}\cdot\text{O4}$ ) listed in Table 2 adds stability to this  $\beta$ -turn fragment.

### Conformation in solution

The flexibility of peptides in solution, in general, is somewhat difficult to determine the conformation. The NMR provides the most reliable information about the structure in solution, provided that an unambiguous assignment of the molecular consti-

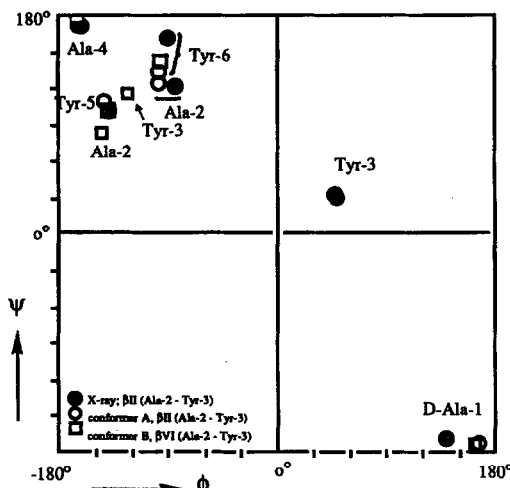


Figure 3 Ramachandran plot,  $\Phi$  and  $\Psi$  angles calculated by X-ray and MD

tion is possible. So, in the following, we will demonstrate the usefulness of high-field NMR spectroscopy for the complete assignments of all C- and all H-signals of conformers A and B (shown in Figure 4) existing in  $\text{CDCl}_3$  solution, by use of the modern two-dimensional techniques.

### Complete assignments of $^1\text{H}$ and $^{13}\text{C}$ NMR signals in conformers A and B

The assignments of  $^1\text{H}$  and  $^{13}\text{C}$ -NMR signals of RA-VII and RA-VII-NMe, shown in Table 3 and 4, were made by the combination of  $^1\text{H}$ - $^1\text{H}$  COSY,  $^1\text{H}$ - $^{13}\text{C}$  COSY and  $^1\text{H}$ - $^{13}\text{C}$  long range COSY (COLOC) spectra. For the assignments on the minor component, conformer B, in particular, HOHAHA spectrum was quite useful. Bates et al.<sup>12</sup> reported the  $^1\text{H}$  and  $^{13}\text{C}$ -NMR spectra of boubardin, the structure of which was closely related to those of RAs, and deduced the structure in solution on the basis of this signal assignments. However, these assignments were turned out to be incorrect and it should be revised, in particular, at the point of the  $^1\text{H}$  chemical shifts of three alanine residues. The conformational determination was performed on the basis of the results of the following experiments.

### Cis/trans isomerism about amide bonds; thermodynamic analysis

It is well known that in such molecules, the rotations about all the bonds except the amide bonds, are too fast to give separate signals in the NMR time scale. Each of the three N-methyl amide bonds of the compound may produce many cis/trans conformers which interconvert at a rate slow enough to give the separate signals. In the  $^1\text{H}$ -NMR spectrum of RA-VII at  $30^\circ\text{C}$ , in an apolar solvent ( $\text{CDCl}_3$ ), the presence of two stable conformational states (A:B=88.6:11.4) was implied. While, in a polar solvent ( $\text{DMSO-d}_6$ ), three conformers (A:B:C=

Table 3  $^1\text{H-NMR}$  Chemical Shifts in  $\text{CDCl}_3$  at 303K (500MHz)

Amino acid	proton	RA-VII		RA-VII-NMe		RA-VII-H	
		major (A)	minor (B)	A	B	major (D)	minor (E)
D-Ala-1	H $\alpha$	4.36 J $\alpha\beta$ =6.9	4.38 J $\alpha\beta$ =6.8	4.73 J $\alpha\beta$ =6.8	4.48 J $\alpha\beta$ =6.7	4.73 J $\alpha\beta$ =6.9	4.40 J $\alpha\beta$ =6.4
	H $\beta$	1.30 J $\alpha\text{N}$ =6.7	1.26 J $\alpha\text{N}$ =7.4	1.25 J $\alpha\text{N}$ =7.0	1.21 J $\alpha\text{N}$ =7.0	1.16 J $\alpha\text{N}$ =6.7	1.24 J $\alpha\text{N}$ =5.4
	HN	6.44	6.41	6.71	6.58	8.03	7.67
Ala-2	H $\alpha$	4.85 J $\alpha\beta$ =6.7	4.82 J $\alpha\beta$ =6.6	5.09 J $\alpha\beta$ =7.2	5.28 J $\alpha\beta$ =6.7	4.34 J $\alpha\beta$ =6.6	4.41 J $\alpha\beta$ =6.8
	H $\beta$	1.35 J $\alpha\text{N}$ =8.4	0.99 J $\alpha\text{N}$ =9.9	1.40	0.96	0.54 J $\alpha\text{N}$ =8.4	1.25 J $\alpha\text{N}$ =5.2
	HN	6.35	6.35			7.41	7.64
	MeN			3.14	3.07		
Tyr-3	H $\alpha$	3.58 J $\alpha\beta$ 1=10.9	4.63 J $\alpha\beta$ 1=10.6	3.55 J $\alpha\beta$ 1=9.5	4.57 J $\alpha\beta$ 1=10.4	5.33 J $\alpha\beta$ 1=11.1	3.59 J $\alpha\beta$ 1=11.5
	H $\beta$ 1(pro-R)	3.34 J $\alpha\beta$ 2=5.0	3.02 J $\alpha\beta$ 2=4.6	3.32 J $\alpha\beta$ 2=6.2	3.03 J $\alpha\beta$ 2=5.2	3.00 J $\alpha\beta$ 2=3.9	3.26 J $\alpha\beta$ 2=4.3
	H $\beta$ 2(pro-S)	3.38 J $\beta$ 1 $\beta$ 2=14.0	3.02	3.34 J $\delta\epsilon$ =8.6	3.03 J $\delta\epsilon$ =8.6	3.00 J $\delta\epsilon$ =8.8	3.37 J $\beta$ 1 $\beta$ 2=13.9
	2H $\delta$	7.04 J $\delta\epsilon$ =8.6	7.09 J $\delta\epsilon$ =8.6	7.05	7.12	7.02	7.04 J $\delta\epsilon$ =8.6
	2H $\epsilon$	6.83	6.84	6.83	6.84	6.82	6.81
	MeN	2.86	2.96	2.85	2.79	2.85	2.84
	MeO	3.79	3.77	3.78	3.77	3.74	3.77
Ala-4	H $\alpha$	4.75 J $\alpha\beta$ =6.9	4.59 J $\alpha\beta$ =6.9	4.80 J $\alpha\beta$ =6.8	4.74 J $\alpha\beta$ =6.9	4.38 J $\alpha\beta$ =7.5	4.77 J $\alpha\beta$ =7.4
	H $\beta$	1.11 J $\alpha\text{N}$ =7.6	1.18 J $\alpha\text{N}$ =7.4	0.98 J $\alpha\text{N}$ =8.3	1.20 J $\alpha\text{N}$ =8.3	1.18 J $\alpha\text{N}$ =5.3	0.94 J $\alpha\text{N}$ =8.2
	HN	6.71	6.68	6.73	6.57	8.62	6.88
Tyr-5	H $\alpha$	5.41 J $\alpha\beta$ 1=11.3	5.41 J $\alpha\beta$ 1=11.3	5.45 J $\alpha\beta$ 1=11.3	5.40 J $\alpha\beta$ 1=11.5	5.35 J $\alpha\beta$ 1= $\alpha\beta$ 2	5.77 J $\alpha\beta$ 1= $\alpha\beta$ 2
	H $\beta$ 1(pro-S)	3.67 J $\alpha\beta$ 2=3.0	3.69 J $\alpha\beta$ 2=3.0	3.70 J $\alpha\beta$ 2=2.8	3.72 J $\alpha\beta$ 2=3.0	2.39	-7.7
	H $\beta$ 2(pro-R)	2.64 J $\beta$ 1 $\beta$ 2=11.4	2.73 J $\beta$ 1 $\beta$ 2=11.4	2.62 J $\beta$ 1 $\beta$ 2=11.3	2.73 J $\beta$ 1 $\beta$ 2=11.5	2.90 J $\beta$ 1 $\beta$ 2=14.0	-----
	H $\delta$ 1	7.26 J $\delta$ 1 $\delta$ 2=2.2	7.26 J $\delta$ 1 $\delta$ 2=2.3	7.26 J $\delta$ 1 $\delta$ 2=2.2	7.27 J $\delta$ 1 $\delta$ 2=2.2	7.29 J $\delta\epsilon$ =7.2	7.28
	H $\delta$ 2	7.42 J $\delta$ 1 $\epsilon$ 1=8.4	7.45 J $\delta$ 1 $\epsilon$ 1=8.4	7.40 J $\delta$ 1 $\epsilon$ 1=8.4	7.44 J $\delta$ 1 $\epsilon$ 1=8.4	7.29 J $\epsilon\zeta$ =7.2	7.28
	H $\epsilon$ 1	6.87 J $\delta$ 2 $\epsilon$ 2=8.4	6.89 J $\delta$ 2 $\epsilon$ 2=8.4	6.86 J $\delta$ 2 $\epsilon$ 2=8.4	6.89 J $\delta$ 2 $\epsilon$ 2=8.4	7.11	7.20
	H $\epsilon$ 2	7.20 J $\epsilon$ 1 $\epsilon$ 2=2.4	7.24 J $\epsilon$ 1 $\epsilon$ 2=2.4	7.20 J $\epsilon$ 1 $\epsilon$ 2=2.2	7.26 J $\epsilon$ 1 $\epsilon$ 2=2.2	7.11	7.20
	MeN	3.13	3.11	3.07	3.06	2.92	2.97
	H $\zeta$					7.11	7.20
Tyr-6	H $\alpha$	4.54 J $\alpha\beta$ 1=12.0	4.60 J $\alpha\beta$ 1=12.0	4.58 J $\alpha\beta$ 1=12.0	4.66 J $\alpha\beta$ 1=12.0	4.80 J $\alpha\beta$ 1=7.9	4.83 J $\alpha\beta$ 1=8.3
	H $\beta$ 1(pro-R)	3.10 J $\alpha\beta$ 2=3.5	3.10 J $\alpha\beta$ 2=3.5	3.13 J $\alpha\beta$ 2=3.8	3.09 J $\alpha\beta$ 2=4.1	2.77 J $\alpha\beta$ 2=7.3	2.90 J $\alpha\beta$ 2=8.3
	H $\beta$ 2(pro-S)	2.95 J $\beta$ 1 $\beta$ 2=18.0	2.95 J $\beta$ 1 $\beta$ 2=18.0	2.91 J $\beta$ 1 $\beta$ 2=2.0	3.01 J $\beta$ 1 $\beta$ 2=15.5	1.88 J $\beta$ 1 $\beta$ 2=13.3	2.37 J $\beta$ 1 $\beta$ 2=15.6
	H $\delta$ 1	6.57 J $\delta$ 1 $\delta$ 2=2.0	6.57 J $\delta$ 1 $\delta$ 2=2.0	6.57 J $\delta$ 1 $\delta$ 2=2.0	6.59 J $\delta$ 1 $\delta$ 2=2.0	6.45 J $\delta$ 1 $\delta$ 2=2.0	6.47 J $\delta$ 1 $\delta$ 2=2.0
	H $\delta$ 2	4.34 J $\delta$ 1 $\epsilon$ 1=8.3	4.34 J $\delta$ 1 $\epsilon$ 1=8.3	4.33 J $\delta$ 1 $\epsilon$ 1=8.4	4.39 J $\delta$ 1 $\epsilon$ 1=8.4	6.58 J $\delta$ 1 $\epsilon$ 1=8.2	6.67 J $\delta$ 1 $\epsilon$ 1=8.2
	H $\epsilon$ 1	6.79	6.80	6.79	6.79	6.55	6.67
	MeN	2.69	2.68	2.74	2.69	3.03	3.06
	MeO	3.93	3.94	3.93	3.94	3.64	3.72

Table 4  $^{13}\text{C}$ -NMR Chemical Shifts in  $\text{CDCl}_3$  at 303K (125MHz)

Amino acid	carbon	RA-VII		RA-VII-NMc		RA-VII-H	
		major (A)	minor (B)	A	B	major (D)	minor (E)
D-Ala-1	C $\alpha$	47.87	47.64	45.85	46.74	49.29	48.77
	C $\beta$	20.67	20.82	18.90	18.85	19.75	19.48
	CC=O	172.23	171.86	172.40	171.17	172.88	172.66
Ala-2	C $\alpha$	44.56	43.67	48.80	48.68	43.88	45.80
	C $\beta$	16.61	16.10	14.33	14.47	16.98	15.87
	CC=O	172.55	171.86	30.94	30.72	173.08	173.00
	CN			30.94	30.72		
Tyr-3	C $\alpha$	68.37	62.14	68.10	61.51	62.63	68.81
	C $\beta$	32.68	33.62	32.64	34.49	33.54	33.06
	C $\gamma$	130.73	130.73	130.85	130.85	129.94	130.81
	C $\delta$	130.24	129.82	130.26	129.75	130.38	130.34
	C $\epsilon$	114.07	114.35	113.99	114.30	114.46	114.00
	C $\zeta$	158.45	158.69	158.36	158.65	158.70	158.39
	CC=O	168.01	168.17	168.34	169.09	167.75	169.87
	CN	39.76	29.86	39.46	29.58	29.19	40.54
	CO	55.26	55.32	55.24	55.24	55.36	55.26
	Ala-4	C $\alpha$	46.43	46.75	46.12	45.41	47.34
C $\beta$		18.50	16.10	18.32	17.77	17.76	18.03
CC=O		171.77	171.32	171.74	170.43	172.18	172.60
Tyr-5	C $\alpha$	54.26	54.72	54.69	55.24	53.98	51.09
	C $\beta$	36.99	36.59	36.90	36.50	35.43	36.64
	C $\gamma$	135.16	135.10	135.52	135.30	136.44	136.54
	C $\delta_1$	132.79	132.79	132.70	132.70	128.49	128.71
	C $\delta_2$	130.98	130.84	130.94	13.94	128.49	128.71
	C $\epsilon_1$	124.24	124.30	124.11	124.27	128.91	128.91
	C $\epsilon_2$	125.91	125.91	125.93	126.00	128.91	128.91
	C $\zeta$	158.25	158.25	158.14	158.25	127.10	126.88
	CC=O	169.33	169.78	168.89	169.48	168.11	171.54
	CN	30.52	30.65	30.56	30.08	31.35	30.17
Tyr-6	C $\alpha$	57.39	57.86	57.10	57.66	61.80	61.44
	C $\beta$	35.52	35.70	35.68	35.58	34.54	34.54
	C $\gamma$	128.18	128.46	128.21	128.38	129.20	129.29
	C $\delta_1$	120.92	120.92	121.04	121.00	120.62	120.56
	C $\delta_2$	113.42	113.59	113.32	113.43	115.48	115.69
	C $\epsilon_1$	112.35	112.35	112.23	112.23	111.23	111.37
	C $\epsilon_2$	153.15	153.15	153.07	153.07	145.69	145.93
	C $\zeta$	146.54	146.54	146.52	146.52	145.82	146.02
	CC=O	170.71	170.62	170.78	169.98	168.98	171.54
	CN	29.28	29.28	29.54	29.44	29.06	29.64
	CO	56.18	56.18	56.12	56.12	55.86	55.96

63.7:31.8:4.5) were suggested to be present in an equilibrium state (See Figure 4). It has been shown that the conversion energy between *cis/trans* isomers about a peptide bond is about 18 kcal/mol<sup>13</sup>. When dissolved in a solvent at low temperatures, it was known to retain its crystalline structure in solution before it isomerized. We dissolved the crystalline of RA-VII from MeOH in CDCl<sub>3</sub> which had been cooled to -60°C and measured the NMR spectrum to correlate the information obtained with the X-ray diffraction data. At -20°C, the main populated conformer A was only detectable as shown in Figure 4. Then, the signals corresponding to those of the minor conformer B appeared upon warming the solution to 5°C.

The thermodynamic parameters of the conversion between the two conformers were determined by the NMR measurements of the conversion rate from conformer A to B. The rate was slow enough to enable the determination to be made by the usual

kinetic method following time-courses at 5°C. The ratios between conformers A and B were determined at intervals of 5 degrees from 0° to 30°C. The rate of the conversion from A to B at 5°C was calculated by the usual first order approach to equilibrium to give the half-life period to be about 7 minutes. From the rate constant at 5°C, the free energy of activation  $G^\ddagger$  was calculated to be 19.6 kcal/mol at 5°C by Eyring equation.<sup>14</sup> The values of enthalpy  $H^\circ$  (6.07 kcal/mol) and the entropy  $S^\circ$  (0.017 kcal/mol K) were also calculated by the rates of populations A and B at each temperature.

#### NOE enhancements

The relationship of NOE enhancements in both conformers A and B of RA-VII are shown in Figure 5. The presence of a type II  $\beta$ -turn in conformer A involving Ala-2 and Tyr-3 was suggested by the enhancement of Ala-2-H $\alpha$  and Tyr-3-H $\alpha$  caused by irradiation of Tyr-3-NCH<sub>3</sub>. In the case of a type I  $\beta$ -turn, detectable NOEs between the above protons are not to be expected. In conformer B, on the other hand, the NOE enhancement between the  $\alpha$ -protons of the adjacent amino-acid residues was observed for Ala-2 and Tyr-3, indicating the peptide bond was *cis*. Likewise, the N-methyl amide bond between Tyr-5 and Tyr-6 was considered to be a *cis* bond by the NOE enhancements observed between Tyr-5-H $\alpha$  and Tyr-6-H $\alpha$  in both conformers. The NOE enhancements between the Tyr-5-NCH<sub>3</sub> protons and Ala-4-CH<sub>3</sub>/Ala-4-H $\alpha$  supported to maintain *trans* in the remaining N-methyl amide bond between Ala-4 and Tyr-5 in both conformers.

The evidences independently provided by one- and two-dimensional NOE measurements in conformer B showed that in conformer B, the peptide bond between Ala-2 and Tyr-3 takes *cis*-conformation which is the sole difference between conformers A and B. Further, the cross peak between the Tyr-3-H $\delta$ , one of the aromatic

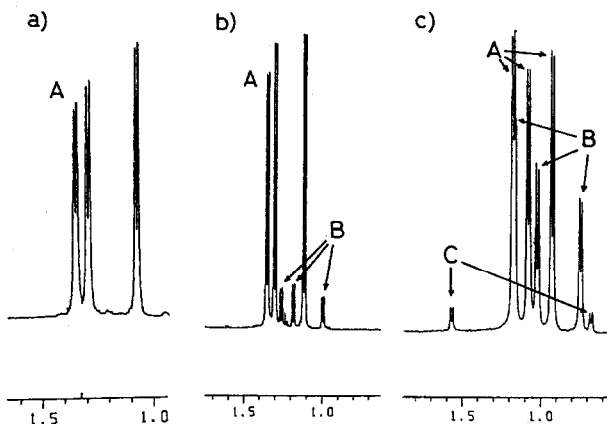


Figure 4 Methyl proton region of <sup>1</sup>H-NMR spectra in RA-VII (500MHz)

- a) Conformer A is only detectable at -20°C in CDCl<sub>3</sub>.
- b) Conformer A and B are shown at 30°C in CDCl<sub>3</sub>.
- c) Three conformers A, B and C at equilibrium state at 30°C in DMSO-d<sub>6</sub>.

protons, and Ala-2-CH<sub>3</sub> in NOESY spectrum suggested that the aromatic side chain, which was considered not to rotate freely, is over the N-methyl amide bond.

In the case of RA-VII-NMe, the similar NOE relationships to those of RA-VII were observed, except for the presence of stronger NOE enhancement between Ala-2-NCH<sub>3</sub> and Ala-2-CH<sub>3</sub> in conformer A than that in conformer B. Therefore, selective methylation of RA-VII is considered to cause steric repulsion between Ala-2-NCH<sub>3</sub> and Ala-2-CH<sub>3</sub> in conformer A.

### Hydrogen bonding

The involvement of NH groups in the intramolecular hydrogen bonding was confirmed on the basis of various data, such as, (1) the temperature effect on the NH chemical shifts in DMSO-d<sub>6</sub>, (2) solvent effect on the NH chemical shifts in CDCl<sub>3</sub>-DMSO-d<sub>6</sub> mixtures and (3) rate of hydrogen-deuterium exchange.

### Temperature dependence of NH chemical shifts

In such a solvent as DMSO-d<sub>6</sub>, the temperature effect on NH chemical shifts is often used to identify the external or internal NH orientations.<sup>15</sup> The temperature coefficients (dδ/dT) of RA-VII and RA-VII-NMe given in Table 5 clearly show that Ala-4-NH is strongly shielded from the solvent, which is characteristic of a proton forming a strong hydrogen bond. It was reported that values  $>3 \times 10^{-3}$  ppm/°C usually suggest solvent-shielded and presumably hydrogen-bonded

NH groups, whereas values  $<4 \times 10^{-3}$  ppm/°C are for exposed groups.<sup>16</sup> The intermediate dδ/dT value for Ala-1-NH does not lead to definitive conclusions. However, the fact that in the case of N-methylation of RA-VII, only Ala-2-NH was predominantly methylated, show that D-Ala-1-NH is shielded from the solvent. On

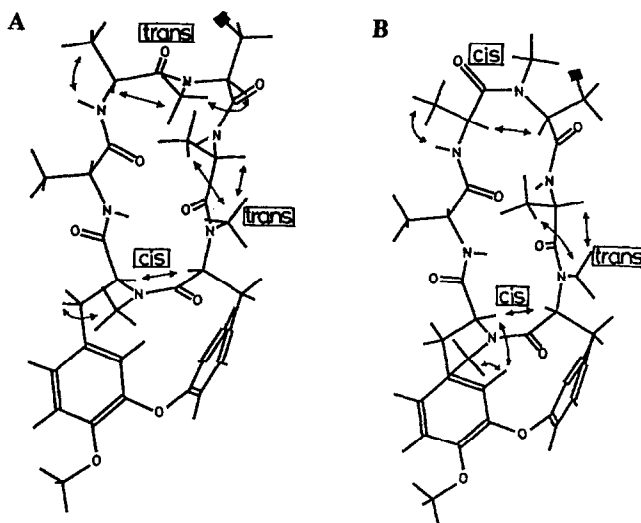


Figure 5 NOE enhancements in conformers A and B of RA-VII. The arrows show the NOE relationships confirmed by 1D-NOE and NOESY experiments in CDCl<sub>3</sub> at 303K.

Table 5 Effect of temperatures on the NH chemical shifts of RA-VII and RA-VII-NMe,  $-\Delta\delta/\Delta T$  ( $10^3$  ppm/K)

Conformers	solvent	D-Ala-1	Ala-2	Ala-4
RA-VII	A DMSO-d <sub>6</sub>	6.0	4.7	0.0
	B DMSO-d <sub>6</sub>	4.3	4.0	0.0
	C DMSO-d <sub>6</sub>	3.7	4.0	0.7
RA-VII	A CDCl <sub>3</sub>	1.1	8.9	0.0
	B CDCl <sub>3</sub>	1.1	10.0	0.9
RA-VII-NMe	A DMSO-d <sub>6</sub>	4.8	----	-0.8
	B DMSO-d <sub>6</sub>	4.8	----	-1.3
	C DMSO-d <sub>6</sub>	3.5	----	-1.0
RA-VII-NMe	A CDCl <sub>3</sub>	0.6	----	0.0
	B CDCl <sub>3</sub>	0.3	----	0.3

the other hand, Ala-2-NH has a  $d\delta/dT$  value characteristic of solvent-exposed NH groups. The temperature coefficients in  $CDCl_3$  listed in Table 5 follow a pattern similar to that in  $DMSO-d_6$ . However, a detailed interpretation of  $d\delta/dT$  values in non-hydrogen bonding solvents like  $CDCl_3$  should be approached carefully because of the association effects,<sup>17)</sup> and we will not elaborate on these results elsewhere.

#### Solvent effect on NH chemical shifts in $CDCl_3$ - $DMSO-d_6$ mixtures

In the solvent titration experiment, Ala-4-NH showed very slight downfield shifts when the concentration of a strongly solvating solvent, e.g.  $DMSO-d_6$  was increased. This suggests that the proton is involved in the hydrogen bonding to support the hypothesis of the presence of a  $\beta$ -turn. On the other hand, the pronounced solvent effect on the Ala-2-NH proton chemical shift shows the complete exposure to the solvent of the Ala-2-NH proton. The slope corresponding to three amide protons was represented in Figure 6.

#### Rates of hydrogen-deuterium (H-D) exchange

A hydrogen-deuterium (H-D) exchange experiment in  $DMSO-d_6$ - $D_2O$  mixtures showed that the exchange half-life times ( $t_{1/2}$ ) for Ala-4-NH, Ala-1-NH and Ala-2-NH were >2days, 6hr and 13min, respectively. These results suggest that Ala-4-NH is involved in a strong intramolecular hydrogen bond, while Ala-1-NH in a weaker hydrogen bond. It must also be considered that these NH groups are sterically shielded by solvent.

#### Side chain conformation

The populations of the side chain rotamers were quantitatively assayed by means of homonuclear coupling constants. The aromatic ring of Tyr-3 shields the Tyr-3-NH<sub>3</sub> hydrogens and the calculated shielding effect closely agrees that obtained from the <sup>1</sup>H NMR spectrum.

The vicinal couplings in the side chain of the Tyr-3 residue in RA-VII, were observed at 10.9 and 5.0Hz in conformer A and at 10.6 and 4.6Hz in conformer B, as given in Table 3. Using the treatment of Pachler,<sup>18)</sup> we calculated the relative populations of the three side-chain rotamers (Fig.7), the results being shown in Table 6. Rotamer I, with  $\chi^1 = -60^\circ$  was the major component as predicted by the calculation as shown later.

In this conformation, the tyrosine side chain is close to the Tyr-3-NH<sub>3</sub> moiety and this methyl protons are expected to be strongly shielded by the aromatic ring of Tyr-3. Calculations, using the atomic coordinates of the calculated structure (See MD and energy minimization section) and the ring-current model of Johnson and Bovey,<sup>19)</sup> showed that in rotamer I, the distance of the Tyr-3-NH<sub>3</sub> hydrogens from the center of the aromatic ring

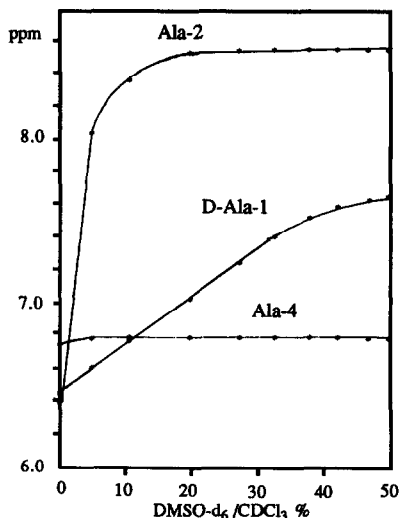


Figure 6 Effect of the concentration of  $DMSO-d_6$  on the NH proton chemical shifts of RA-VII

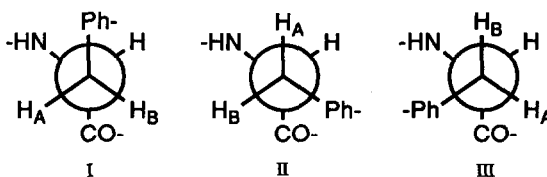


Figure 7 Rotamers about the  $C\alpha - C\beta$  bond axis for Tyr-3



were 3.76Å in conformer A and 3.87Å in conformer B, and that such hydrogens should experience shielding of 0.46 and 0.19ppm,

Table 6  $^1\text{H-NMR}$  parameters for Tyr-3 side chain in conformers A and B of RA-VII and the % of rotamers in  $\text{CDCl}_3$ .

	Coupling constants (Hz)			Rotamer populations (%)		
	J <sub>AB</sub>	J <sub>AX</sub>	J <sub>BX</sub>	I	II	III
Conformer A	14.0	10.9	5.0	75.7	21.9	2.4
Conformer B	— <sup>a)</sup>	10.6	4.6	73.0	18.3	8.7

a) Not determined

respectively. Since this shielding was observed in 76% and 73%, respectively of rotamers I, the resultant shielding effects are 0.35 and 0.14ppm, respectively. The chemical shifts of Tyr-5-NCH<sub>3</sub> hydrogens which was free from anisotropic effect were 3.13 in conformer A and 3.11ppm in conformer B, in RA-VII. Therefore, because of this shielding effect, the chemical shift of the Tyr-3-NCH<sub>3</sub> hydrogens would be 2.78 and 2.97ppm, respectively. As shown in Table 3, these signals appeared at 2.86 and 2.96ppm, respectively, which confirmed the assignments were correct and that their actual positions were very close to that predicted by the calculation.

### $^{13}\text{C}$ -chemical shift of Tyr-3 and structure of conformer C in solution

The  $^{13}\text{C}$  chemical shifts of polypeptides exhibit considerable effect of conformations such as  $\alpha$ -helix and  $\beta$ -sheet forms<sup>20)</sup> on  $^{13}\text{C}$  chemical shifts. It appears that such conformational effect on  $^{13}\text{C}$  shifts are mainly caused by the different local conformation of individual amino acid residues having different dihedral angles ( $\phi$  and  $\psi$ ) and different intra- or intermolecular hydrogen bondings.<sup>21)</sup>

The significant lowerfield shift of Tyr-3-C $\alpha$  in conformer A, compared with the corresponding shift in minor conformer B, agrees with those observed in  $\alpha$ -helix type peptides<sup>22)</sup> and supports the proposed type II  $\beta$ -turn in the residues between Ala-2 and Tyr-3.

On the other hand, the chemical shift of Tyr-3-C $\alpha$  in conformer C, appearing in DMSO- $d_6$  was almost the same as that of conformer B. This fact suggested that in conformer C, conformation isomerized about Ala-2 and Tyr-3 amide bond also dominated. Then, NOE enhancement between Tyr-5-NCH<sub>3</sub> and Tyr-5-H $\delta$  in the NOESY spectrum indicated the isomerization to cis of Ala-4 - Tyr-5 amide bond, and therefore, the three N-methyl amide bonds were shown to be in cis orientation. This was also supported by the lower field shift ( $\delta$ 1.57) of Ala-4-CH<sub>3</sub> caused by the deshielding effect of aromatic ring in Tyr-5.

### Solution structure and activity of RA-VII-H

Hydrogenolysis of RA-VII with PtO<sub>2</sub> gave RA-VII-H having no diphenyl ether bond and no antitumor activity. Two stable conformers, named conformers D and E were observed in  $\text{CDCl}_3$  in a ratio of 66.7 : 33.3. Complete assignments of the  $^1\text{H}$ - and  $^{13}\text{C}$ -signals by the homo and heteronuclear 2D-NMR techniques as shown in Tables 3 and 4, NOE enhancements and temperature effect on the NH chemical shifts suggested that the backbone amide bonds of minor conformer E has the same geometrical conformation as that of conformer A. In the major conformer D, however, all the three N-methyl amide bonds were

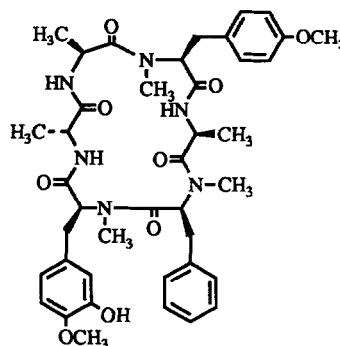


Figure 8 Structure of RA-VII-H given by hydrogenolysis of RA-VII



strong negative Cotton effect at 235nm ( $\Delta\epsilon=-22.30$ ). This spectrum is indicative of a rigid peptide backbone.<sup>25</sup> The weak positive curve at about 270nm became negative at +20°C. Since the three tyrosyl residues, Tyr-5, Tyr-6 and Tyr-3 were located quite apart from each other in the molecule, the interactions among them might be ignored: only the interactions between the tyrosyl and the amide (Tyr-3 and the N-methyl amide constructed by Ala-2 and Tyr-3) need to be taken into consideration. This change of the sign at about 270nm was considered to be caused by the interactions between the Tyr-3 absorption bands at 277 and 227nm and the amide  $n-\pi^*$  and  $\pi-\pi^*$  transitions.

### Molecular dynamics and energy minimization

In order to obtain a more detailed structure and conformations which agrees more closely with the NMR data, we performed the molecular dynamics calculations starting with X-ray structure and applying the distance constraints obtained from the NMR experiments. The final structures obtained after several such calculations were examined for the overall energetic favorability and compared with the structure derived from the NMR data.

The AMBER program system<sup>26</sup> was used for the constrained energy minimization and molecular dynamics optimization of the structures in the following manner. The starting coordinates of RA-VII were taken from the X-ray structure of RA-V-*p*-bromobenzoate with removal conversion of the *p*-bromobenzoate. After the energy minimization, we performed a 100psec restrained MD run. The MD run consisted of 0.5fs time step at 1000K with a strong coupling to the temperature bath.<sup>27</sup> The amide bond between Tyr-5 and Tyr-6 was fixed in the *cis* geometry, as also found in the solid-state conformation. The similarity of this geometry in solution state was also investigated by the intensive NOESY correlations observed between Tyr-5-H $\alpha$  and Tyr-6-H $\alpha$  in both conformers A and B. The side chain of Tyr-3 is flexible and gives large fluctuation to the total energy corresponding to its different conformations. In order to discriminate between conformational energy of the hexapeptide ring and conformational energy of the Tyr-3 side chain, calculation was made with a hypothetical compound in which Tyr-3 was replaced by alanine (Figure 11: The structure having the type II  $\beta$ -turn was stabler by 2.26kcal than that being the type VI  $\beta$ -turn.). Conformation of the Tyr-3 side chain was simulated separately as described below.

### Structure of conformer A

It is obvious from the calculated dihedrals (See Table 7) and the Ramachandran plot shown in Figure 3 that the conformation of the type II  $\beta$ -turn structure is fulfilled for conformer A, the structure of which involves Ala-2 in the *i*+1 and Tyr-3 in the *i*+2 positions by stabilization of the transannular H-bridge between Ala-4-NH and Ala-1-CO. In conformer A, two NOE enhancements, i.e. one between Ala-2-H $\alpha$  and Tyr-3-NCH<sub>3</sub> and one between Tyr-3-NCH<sub>3</sub> and Tyr-3-H $\alpha$  were observed which gives another evidence for the assumption of the described type II  $\beta$ -turn structure. The Ramachandran plots in Figure 3 indicates that the degree of deviations of the MD-calculated torsion values from the ideal values are similar for RA-VII and RA-VII-NMe.

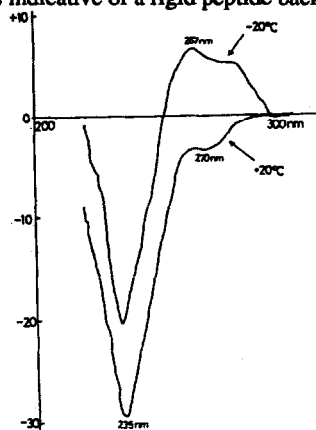


Figure 10 CD curves of RA-VII in CHCl<sub>3</sub>

### Structure of conformer B

The solution structure of the minor conformer B of RA-VII and that of VII-NMe were not so definitely determined as that of conformer A, because no sufficient NOE values were available. None of the  $\beta$ -turns are retained in this conformer which can be realized from the Ramachandran plots in Figure 3 where the values of the dihedrals are included. The type II  $\beta$ -turn involving Ala-2 in the  $i+1$  and Tyr-3 in the  $i+2$  position is converted to a type VI  $\beta$ -turn-type structure<sup>28</sup>), which is determined by the NOE enhancements between Ala-2-H $\alpha$  and Tyr-3-H $\alpha$  indicating a *cis* peptide bond. A similar type VI  $\beta$ -turn determined by an NOE between H $\alpha$  protons was already observed for the weakly populated conformer of VDA 008<sup>29</sup>) and [Ne-L-Leu]didemnin B<sup>30</sup>), each cyclic hexapeptide.

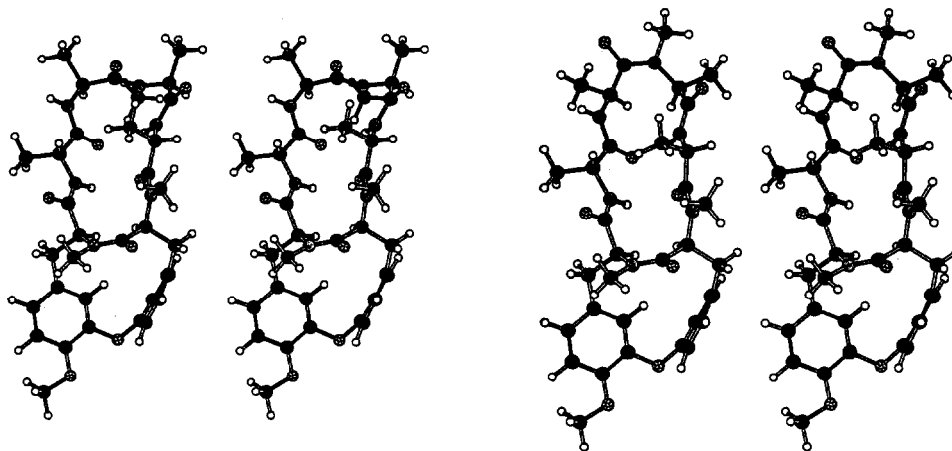


Figure 11 Stereoscopic view of two stable backbone structures of the hypothetical compound in which Tyr-3 of RA-VII is replaced by alanine given by MD and energy minimizations

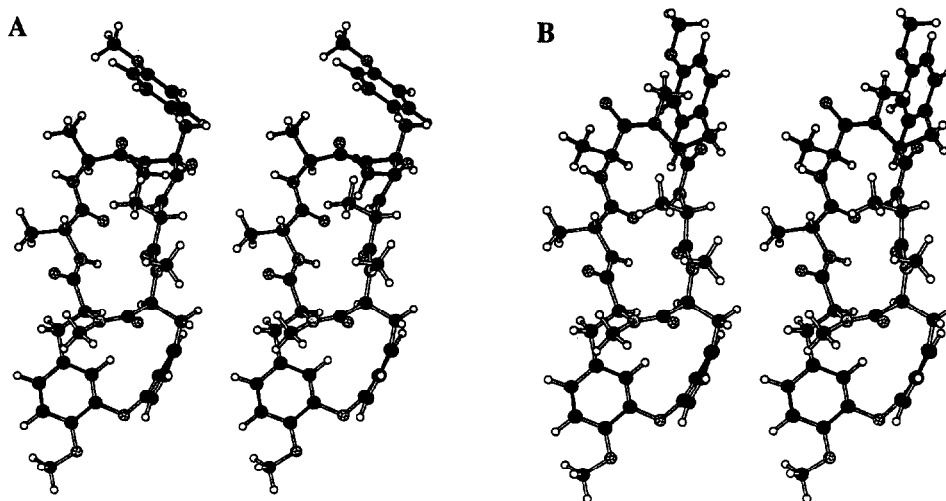


Figure 12 Stereoscopic view of two stable conformers corresponding to the conformers A and B given by energy maps

In conformer B of RA-VII-NMe, the bond distance (3.175Å) between the carbon of Ala-2-CH<sub>3</sub> and that of Ala-2-NCH<sub>3</sub> is remote in comparison to that (2.885Å) in conformer A. This difference may account for the reduction in the % of conformer A in RA-VII-NMe.

### Side chain conformation

After minimization of backbone structure, the stable conformers A and B involving in the side chain of Tyr-3 were obtained by the energy maps calculated by the rotates of  $\chi_1$  and  $\chi_2$  per 5 degrees (Figure 12).<sup>31)</sup> The conformation of A approximately corresponds to that of the crystalline and both conformers A and B were found to be identical to the solution conformations analyzed by homonuclear coupling constants, calculated populations and the shielding effect of Tyr-3 as described above (See solution conformation).

Table 7 X-ray- and MD-calculated backbone dihedrals in RA-VII and RA-VII-NMe

Residue	Dihedral angle	RA-VII		RA-VII-NMe		X-ray <sup>a)</sup>
		conformer A	B	A	B	
D-Ala-1	$\phi$	168	166	169	155	139
	$\psi$	-173	-173	-169	-151	-168
	$\omega$	-180	-172	-177	-171	-175
Ala-2	$\phi$	-70	-124	-79	-134	-83
	$\psi$	117	87	123	78	121
	$\omega$	-172	1	-170	4	-178
Tyr-3	$\phi$	52	-108	53	-117	54
	$\psi$	38	113	38	61	39
	$\omega$	-177	179	-178	166	-168
Ala-4	$\phi$	-157	-160	-158	-75	-159
	$\psi$	168	177	167	172	170
	$\omega$	-178	173	-178	174	175
Tyr-5	$\phi$	-127	-118	-126	-113	-137
	$\psi$	104	103	104	103	101
	$\omega$	-8	-8	-8	-8	1
Tyr-6	$\phi$	-85	-85	-85	-84	-92
	$\psi$	131	137	132	152	162
	$\omega$	165	165	164	172	171

a) The data of X-ray diffractometry indicate the angles in RA-V-p-bromobenzoate

### Conclusion

This study showed that the conformers A and B of RA-VII are trans-cis isomers about the Ala-2-Tyr-3 peptide bond. Cis-trans isomerism about the amide bond was the first problem effectively studied by dynamic NMR spectroscopy.<sup>32)</sup>

When the Ala-2 residue of RA-VII was N-methylated, only the conformation of the amide bond of conformer A involved in the type II  $\beta$ -turn changed. However, the biological activity of RA-VII-NMe was considerably lower than that of RA-VII.<sup>33)</sup> The reduction in the % of conformer A in RA-VII-NMe may account for the reduction of the activity of RA-VII-NMe. The small change in the backbone conformation may be sufficient to reduce the receptor binding ability of RA-VII-NMe in comparison to that of RA-VII. However, it is difficult to rule out completely the following possibility that structural change between RA-VII and RA-VII-NMe causes the reduction of the activity.

On the other hand, the solution conformation of the reductive hexapeptide lacking the diphenyl ether bond (RA-VII-H) was suggested to be the mixture of different conformers D and E, whose population of type II  $\beta$ -turn was reversed and also may be responsible for the lack of the activity.

## Experimental

Proton and carbon spectra were recorded on Bruker spectrometers (AM400 and AM500) and processed on a Bruker data station with an Aspect 3000 computer. The 8mg sample of RA-VII, VII-NMe and VII-H in a 5mm tube (0.5ml CDCl<sub>3</sub> or DMSO-d<sub>6</sub>, degassed) was used for the homonuclear, and 30mg sample of RA-VII, VII-NMe and VII-H in a 5mm tube (0.5ml CDCl<sub>3</sub> or DMSO-d<sub>6</sub>, degassed) for the heteronuclear measurements. The spectra were recorded at 303K.

### NOE

NOESY experiments were acquired with mixing times of 0.4, 0.6 and 0.8s. Structural assessments utilized values from the 0.6s experiments, since no secondary effects were observed at this mixing time.

### T1 relaxation times (100MHz)

All spectra were recorded on a Bruker AM400 spectrometer at 100.6MHz using proton broad-band decoupling at 303K. The spectra contained 32K data points over a 24KHz frequency range. Relaxation data were obtained by using the inversion-recovery 180- $\tau$ -90° pulse sequence. Repetition time between two acquisitions was 60s for RA-VII in CDCl<sub>3</sub>. The spin-lattice relaxation times were determined from the relaxation data by using a regression analysis that was incorporated in the T1 routine of the Bruker acquisition and processing program and given by the expression  $Y=A_3 + A_2 \cdot \exp(-t/T_1)$  in which A<sub>3</sub> and A<sub>2</sub> are constants and represents the delay times between the 180° and 90° pulses. For the calculation of T<sub>1</sub>, we used the relative intensities of the <sup>13</sup>C signals at 15 different values in an appropriate range, standard deviations were in the range of 0.006 to 0.052s.

### Molecular dynamics and molecular mechanics calculations

Computer modeling was carried out with the MOL-GGRAPH program system (ver. 2.0) on an AIRIS 4-D workstation. Initial calculations started with coordinates for the X-ray structure of the p-bromobenzoate derivative of RA-V. Molecular mechanics and dynamics calculation were performed with the AMBER 3.0 package<sup>34)</sup> with a distance-dependent dielectric,  $\epsilon=R_{ij}$ . Considering the NOE between Ala-2-H $\alpha$  and Tyr-3-H $\alpha$ , and two intramolecular hydrogen bondings of NH<sub>4</sub>-O<sub>1</sub> and NH<sub>1</sub>-O<sub>4</sub>, constrained minimizations and dynamics were calculated with an extra harmonic term of the form  $E=\sum K(r-r_{\max})^2$  for  $r>r_{\max}$  and  $E=0.0$  for  $r<r_{\max}$  added to the force field (NOE: 3.0Å<sup>></sup>, K=5kcal·Å<sup>-2</sup>; H-bondings: 3.5Å<sup>></sup>, K=5kcal·Å<sup>-2</sup>). Relevant solution-phase conformations were predicted by a general method described below. In order to discriminate between conformational energy of the hexapeptide ring and conformational energy of the Tyr-3 side chain, calculation was made with a hypothetical compound in which Tyr-3 was replaced by alanine. Molecular dynamics at 1000K for a total of 100psec were calculated with a time step 0.5fsec and structures were sampled every 0.1psec. The snapshots from the dynamics trajectories were then energy minimized. A snapshot with the lowest energy was selected as an relevant conformation.

### CD

Circular dichroism was measured with 0.1mm cell in CHCl<sub>3</sub> by JASCO-500C spectropolarimeter. The absorption cell was thermostated at -20°C and then increased temperature up to +20°C. Results are reported as  $\Delta\epsilon$  values.

### RA-VII-NMe

RA-VII was stirred with iodomethane and FK/Al<sub>2</sub>O<sub>3</sub><sup>35)</sup> in 1,2-dimethoxyethane at room temperature for 15hr. The reaction mixture was filtrated and then concentrated to give RA-VII-NMe quantitatively.

**RA-VII-H**

RA-VII (100mg) was hydrogenated with PtO<sub>2</sub> in CHCl<sub>3</sub>-MeOH-AcOH (2:1:2) solution for 6hr. The reaction mixture was purified by ODS-HPLC (80%MeOH) to give RA-VII-H (22mg).

**X-ray analysis of RA-V-*p*-Br-benzoate**

Crystal data: C<sub>47</sub>H<sub>51</sub>N<sub>6</sub>O<sub>10</sub>BrC<sub>2</sub>H<sub>5</sub>OH<sub>2</sub>H<sub>2</sub>O, monoclinic, space group P2<sub>1</sub>, z=2, a=27.874(15), b=9.653(6), c=9.758(6)Å, β=95.77(6)°, V=2612Å<sup>3</sup>. A total of 2017 reflections were observed as above the 2σ (I) level within the 2θ range from 6° through 90°. The structure was determined by the heavy atom method coupled with the anomalous dispersion method. The latter was of use for eliminating the pseudo-mirror, 010 plane through the bromine atom. The refinement was carried out by the method of block-diagonal-matrix least-squares. The final R value was 0.096 for 2017 reflections assuming anisotropic thermal vibrations for 69 atoms excluding hydrogen.

**References and Notes**

- 1) 32th SYMPOSIUM on THE CHEMISTRY OF NATURAL PRODUCTS, CHIBA, SYMPOSIUM PAPERS pp72-78.
- 2) H. Itokawa, K. Takeya, K. Mihara, N. Mori, T. Hamanaka, T. Sonobe and Y. Iitaka, Chem. Pharm. Bull., 1983, 31, 1424.
- 3) H. Itokawa, K. Takeya, N. Mori, T. Hamanaka, T. Sonobe and K. Mihara, Chem. Pharm. Bull., 1984, 32, 284; H. Itokawa, K. Takeya, N. Mori, T. Sonobe, S. Mihashi and T. Hamanaka, *ibid.*, 1986, 34, 3762.
- 4) H. Itokawa, K. Takeya, N. Mori, S. Kidokoro and H. Yamamoto., Plant Med., 1984, 50, 313; H. Itokawa, K. Takeya, N. Mori, M. Takanashi, H. Yamamoto, T. Sonobe and S. Kidokoro, Gann, 1984, 75, 929.
- 5) T. Inaba, I. Umezawa, M. Yuasa, T. Inoue, S. Mihashi, H. Itokawa and K. Ogura, J. Org. Chem., 52, 2957 (1987).
- 6) H. Itokawa, K. Takeya, T. Hamanaka, M. Takanashi, N. Mori and S. Tsukagoshi, Recent Advances in Chemotherapy, Anticancer Section, Proceedings of the 14th International Congress of Chemotherapy, Kyoto, 643 (1985).
- 7) H. Itokawa, K. Takeya, N. Mori, T. Sonobe, N. Serisawa, T. Hamanaka and S. Mihashi, Chem. Pharm. Bull., 1984, 32, 3216.
- 8) G. R. Kriek, Dissertation Abstracts International, 1980, 41, 572-B, 573-B; R. B. Bates, S. L. Gin, H. A. Hassen, V. J. Hrubby, K. D. Janda, G. R. Kriek, J-P Michaud and D. B. Vine, Heterocycles, 1984, 22, 785.
- 9) Recent examples; a) H. Kessler, U. Anders and M. Schudok, J. Am. Chem. Soc., 1990, 112, 5908; b) V. J. Hrubby, L-F Kao, B. M. Pettitt and M. Karplus, J. Am. Chem. Soc., 1988, 110, 3351; c) W. Inman and P. Crews, J. Am. Chem. Soc., 1989, 111, 2822; H. Kessler, J. W. Bats, C. Griesinger, S. Koll, M. Will and K. Wagner, J. Am. Chem. Soc., 1988, 110, 1033; e) S. W. Fesik, G. Bolis, H. L. Sham and E. T. Olejniczak, Biochemistry, 1987, 26, 1851.
- 10) Final crystallographic coordinates and the structure factor table have been deposited in the Cambridge Crystallographic Data Center.

- 11) W. R. Chan, W. F. Tinto, P. S. Manchand and L. J. Todaro, *J. Org. Chem.*, 1987, 52, 3091.
- 12) R. B. Bates, J. R. Cole, J. J. Hoffmann, G. R. Kriek, G. S. Linz and S. T. Torrance, *J. Am. Chem. Soc.*, 1983, 105, 1343.
- 13) W. E. Stewart, T. H. Siddall, *Chem. Rev.*, 1970, 70, 517; H. Kessler, *Angew. Chem.*, 1970, 82, 237; *ibid.*, Int. Ed., 1970, 9, 219; S. Sternhell, "Dynamic Nuclear Magnetic Resonance", Eds. L. M. Jackman and F. A. Cotton, Academic Press, New York, 1975, 163.
- 14) H. Gunther, "NMR Spectroscopy"; Wiley; New York, 1980; pp 240-244.
- 15) H. Kessler, *Angew. Chem.*, 1982, 94, 509; *ibid.*, Int. Ed., 1982, 21, 512.
- 16) M. Iqbal and P. Balaram, *Biopolymers*, 1982, 21, 1427.
- 17) E. S. Stevens, N. Sugawara, G. M. Bonara, C. Toniolo, *J. Am. Chem. Soc.*, 1980, 102, 7048.
- 18) K. G. R. Pachler, *Spectrochim. Acta*, 1964, 20, 581.
- 19) C. E. Johnson and F. A. Bovey, *J. Chem. Phys.*, 1958, 29, 1012.
- 20) A. E. Tonelli, *J. Am. Chem. Soc.*, 1980, 102, 7635; A. Shoji, T. Ozaki, H. Saito, R. Tabeta, I. Ando, *Macromolecules*, 1984, 17, 1472.
- 21) I. Ando, H. Saito, R. Tabeta, A. Shoji, T. Ozaki, *Macromolecules*, 1984, 17, 457.
- 22) H. Saito, R. Tabeta, I. Ando, T. Ozaki and A. Shoji, *Chem. Lett.*, 1983, 1437.
- 23) A. Allerhand, D. Doddrell and R. Komoroski, *J. Chem. Phys.*, 1971, 55, 189; J. R. Lyerla and G. C. Levy, *Top. carbon-13 NMR Spectrosc.* 1974, 1, 79-148.
- 24) Yu. A. Ovchinnikov and V. T. Ivanov, *Tetrahedron*, 1975, 31, 2177.
- 25) C. A. Bush and D. E. Gibbs, *Biochemistry*, 1972, 11, 2421.
- 26) P. K. Weiner and P. A. Kollman, *J. Comput. Chem.*, 1981, 2, 287.
- 27) H. J. C. Berendsen, J. P. M. Postma, W. F. van Gunsteren, A. DiNola, J. R. Haak, *J. Chem. Phys.*, 1984, 81, 3684.
- 28) G. D. Rose, L. M. Gierasch, J. A. Smith, *Adv. Protein Chem.*, 1985, 37, 1.
- 29) U. Anders, Dissertation, Frankfurt, 1989, pp 98.
- 30) H. Kessler, S. Mrouga, M. Will, U. Schmidt, *Helv. Chim. Acta*, 1990, 73, 25.
- 31) The energy maps were made by use of Lennard-Jones potential in the MOLGRAPH program system.
- 32) W. D. Phillips, *J. Chem. Phys.*, 1955, 23, 1363; H. S. Gutowski and C. H. Holm, *J. Chem. Phys.*, 1956, 25, 1228.
- 33) Optimun dose against P-388 leukemia; (T/C %)

	RA-VII	RA-VII-NMe
<i>i.p.</i>	4 mg/kg (234%)	10 mg/kg (172%)
<i>i.v.</i>	6 mg/kg (167%)	9 mg/kg (158%)

- 34) P. K. Weiner and P. A. Kollman, *J. Comput. Chem.*, 1981, 2, 287.
- 35) T. Ando, J. Yamawaki, T. Kawate, S. Sumi and T. Hanafusa, *Bull. Chem. Soc. Jpn.*, 1982, 55, 2504; T. Ando, S. J. Brown, J. H. Clark, D. G. Cork, T. Hanafusa, J. Ichihara, J. M. Miller and M. S. Robertson, *J. Chem. Soc. Perkin trans. II*, 1986, 1133.